Extending the self-assembly of coiled-coil hybrids

Robson, M.H.

UNDERSTANDING THE BINDING OF THE E/K PEPTIDE DIMER IN AQUEOUS SOLUTION, A COMBINED EXPERIMENTAL AND COMPUTATIONAL STUDY

Coiled coils are composed of α-helical peptides that bind together with an affinity and specificity that is very sensitive to the amino acid sequence. This potential to link the amino acid sequence to peptide form and function makes them valuable building blocks for nanostructures with novel functions. The design criteria for coiled coils are relatively well understood, though still incomplete, therefore to maximize their use in supramolecular chemistry it is important to extend the general design criteria to an understanding of the contribution of each amino acid to the coiled-coil binding. In this Chapter experimental techniques are combined with molecular dynamics simulations to quantify the parallel coiled-coil heterodimer formation of the peptides E and K. It is shown firstly that the simulations accurately predict the peptide tertiary and quaternary structures; and secondly, by breaking down the binding energy of each amino acid, that the simulations provide useful insights into the importance of particular residues to the coiled-coil binding. For example, the van der Waals energies of the terminal core forming residues drive the binding of E and K, while the charged residues bordering the core, contrary to previous assumptions, destabilize the dimer. K is optimally designed, but E is energetically more favorable in monomeric form, hence the sequence could be redesigned to stabilize the heterodimer. The computational results complement and extend the experimental results, demonstrating that this method will be useful to connect peptide sequence to the function of complex designed coiled-coil building blocks.

INTRODUCTION

Coiled coils consist of α-helical peptides that fold together due to shielding of hydrophobic residues and through electrostatic interactions between charged residues on adjacent coils.[1] The archetypal coiled-coil forming sequence has a heptad repeat of amino acids, represented by **abcdefg**, with positions **a** and **d** being hydrophobic residues that form a 'hydrophobic face' when the peptide is in the α-helical conformation.[2] The packing of two or more of these hydrophobic faces together results in the helices wrapping around one another in a left-handed supercoil.[3] In this conformation the charged amino acids **e** and **g** border the core, and the electrostatic attractions or repulsions between these confer alignment and specificity to a particular combination of helices (Figure 1).[2] The noncovalent association of the peptides is sensitive to changes in pH, temperature and salt content.[4-7]

The coiled-coil motif is a common structure in nature, with up to 10% of eukaryotic proteins containing sequences predicted to adopt the coiled-coil motif.[8] The coiled-coil domain has a diverse array of functions in different proteins, for example acting as spacers between functional head and tail domains, forming filaments and networks, operating as flexible connectors, tethering vesicles, facilitating membrane fusion, and acting as temperature sensors by unfolding above a certain temperature.[9] Because of the response of coiled coils to changes in the cellular environment it is expected that more regulatory functions of the coiled-coil motif will be discovered. In natural coiled coils there can be some variation in the placement of hydrophobic, hydrophilic, and neutral residues at certain positions in the heptad repeat, and indeed some variation could be essential to balance the need for both stability and specificity.[10, 11]

The coiled-coil motif is on one hand very simple – it is a cylinder with well defined size, shape, and surface functionality, it consists only of α-helix secondary structure, and is readily identified by circular dichroism; and on the other hand the binding properties can be controlled through design of the amino acid sequence and also post-synthesis by external stimuli such at temperature, salt and pH.[4-7] This combined simplicity and functionality has lead to their use as 'natural' molecular tools in nanotechnology. Applications of coiled coils to date include those in the bionanotechnology field, such as affinity purification and biosensors,[12] conformationally defined combinatorial libraries,[13] the directed assembly of extracellular receptor domains,[14] and the creation of miniature antibodies.[15] A burgeoning area of interest is their incorporation into hybrid macromolecules, as their well-defined structure and responsiveness allow precise control over nano-, micro-, and macrostructure. Examples are hydrogels,[16-18] controlled aggregation of gold nanoparticles,[19] the formation of fibers[20-23] and fractal structures,[24] incorporation into hierarchically self-assembling block copolymers,[25] and in liposome fusion systems.[26]

With this increasing complexity of biomaterials that incorporate coiled coils the peptides are not acting in isolation, the binding properties – stability, specificity, aggregation number, and orientation – are also influenced by the self assembly of neighboring groups. The current coiled coil design rules have been sufficient for a number of applications, but as seen in nature, there are numerous functions that they can undertake, and in order to make full use of the potential of coiled coils in biomaterials there is a need for a quantitative measure of the coiled-coil binding.

This Chapter combines experimental and computational results to understand in greater detail why one peptide dimer 'binds' while another will not by looking at the contributions of each amino acid in the heptad repeat in a quantitative way, beyond the 'hydrophobic', 'neutral', or 'hydrophilic' qualifications. The van der Waals and coulomb contributions of each residue to the dimer binding is calculated. This is the first time that the contributions of each amino acid to coiled-coil binding have been presented.

It is demonstrated that these computational techniques can use amino acid sequences as input and from these accurately calculate the intermolecular structural and binding properties of coiled-coil forming peptides. These techniques can now be used to predict the binding in more complex applications of coiled-coil forming peptides, for example peptide containing hybrids, which will focus advances in this expanding field.

RESULTS AND DISCUSSION

Peptide design

The peptide sequences used in this study are based on an α-helical coiled-coil pair shown by Litowski and Hodges to exclusively form parallel heterodimers with high conformational stability.[27-30] The compositions of the peptides are shown in Table 1. At three heptad repeats they are amongst the shortest peptides that form stable coiled-coil heterodimers.

Table 1. Peptide sequences.

Name	Structure[a]	M_n[b]
K	Ac-WG(KIAALKE)$_3$G-NH$_2$	2620
E	Ac-YG(EIAALEK)$_3$-NH$_2$	2543

[a] Ac = acetyl. The sequences are written using the one-letter amino acid code. [b] M_n (molecular weight) values of the hybrid molecules were calculated from MALDI-TOF spectra.

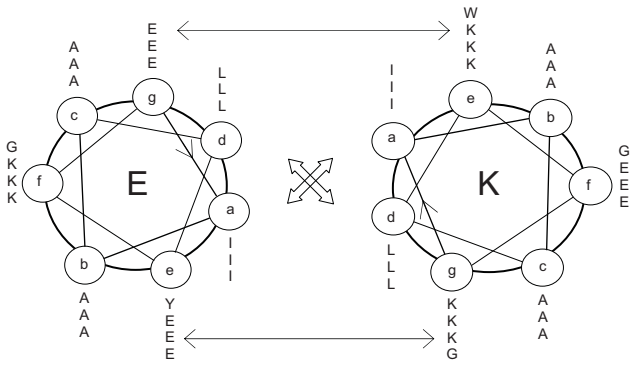

Figure 1. Helical wheel diagram of peptides E and K. Peptides E and K propagate into the page from the N-terminus to the C-terminus. The potential inter-helical electrostatic interactions are demonstrated by thin arrows and the inter-helical hydrophobic core packing by open arrows.

This pair incorporates design criteria for each position in the heptad repeat (Figure 1) in order to maximize the stability of the parallel heterodimeric α-helical coiled coil. The hydrophobic core (positions **a** and **d** in the amino acid heptad repeat), has been found previously to be most stabilized by β-branched amino acids at position **a** [31], in this case isoleucine, and that leucine is the most stabilizing residue at position **d,**[32] as is the case with these peptides. This combination of isoleucine and leucine in the hydrophobic core sterically fit well together in a 'knobs in holes' manner.[27]

Heterodimerization was programmed by incorporating charged residues at positions **e** and **g**, bordering the hydrophobic core, with these being lysine for peptide K and glutamic acid for peptide E. The experiments are carried out at pH 7.0, where the side chains of all lysine residues should be protonated, and hence positively charged, and the side chains of all glutamic acid residues should be deprotonated and hence negatively charged.[33] In this way it is thought that homodimers are destabilized by electrostatic repulsions and heterodimers are stabilized by electrostatic attractions. The peptides used in this study

were based on a pair that were three heptad repeats long. The individual peptides did not form homodimers, but when combined they formed heterodimers. Peptides were also synthesized with four heptad repeats and these did self-associate,[28] demonstrating the fine balance required between the stabilization provided by the hydrophobic core and the specificity imparted by the charged amino acids at these side positions.

Positions **b** and **c** , away from the hydrophobic face, were occupied by alanine residues, which are known to increase the likelihood that a peptide adopts an α-helical configuration.[34]

The final position in the heptad repeat, position **f**, was occupied by either lysine or glutamic acid, the opposite of what is in positions **e** and **g**, thus decreasing the overall net charge on a single peptide and increasing the solubility.[28]

The peptides also include N-terminal fluorescent amino acids tryptophan and tyrosine to enable characterization of the peptide orientation (parallel or antiparallel) by fluorescence spectroscopy. These are separated from the three heptad repeats by a glycine spacer to reduce possible end-fraying effects of the tryptophan and tyrosine. Peptide E also has a C-terminal glycine residue to act as a spacer between the peptide and polymers in future hybrid studies.[25]

First the experimental results are discussed in terms of peptide structure and binding, followed by the results from the computer simulations, again divided into structural and binding properties.

Experimental Results – Structural Properties

Circular Dichroism.

Peptide E has a predominantly random coil structure in phosphate buffered saline (PBS, pH 7.0), while K is predominantly α-helical, as determined by their circular dichroism (CD) spectra (Figure 2a). With an equimolar mixture of E and K, denoted E/K, the intensity at 222 nm, which is directly proportional to the amount of helical structure, [35] increased. The ellipticity ratio, $[\theta]_{222}/[\theta]_{208,}$ also increased to 1.01 (Table 1), indicative of the formation of coiled coils.[36]

The peptide interaction was further analyzed by recording CD spectra after diluting the samples 1:1 (v/v) with trifluoroethanol (TFE). TFE is known to enhance intramolecular α-helicity while disrupting intermolecular interactions.[37] In this solvent mixture the % α-helicity of E and K increased and their ellipticity ratios were 0.80 and 0.81 respectively, which is in the range of monomeric helices. For the mixture there is a significant decrease in the $[\theta]_{222}/[\theta]_{208}$ ratio from benign buffer to 50% TFE, decreasing from 1.01 to 0.81, as the intermolecular coiling is destabilized and single coils with the same % α-helicity as the individual peptides are formed (Table 1).

These results confirm that individually the peptides do not self associate, which is due to electrostatic repulsions overcoming the stability provided by the forming of the hydrophobic core. When the peptides are combined they assemble into hetero coiled coils

as the electrostatic interactions no longer negate the stability provided by the hydrophobic core. These results are in accordance with the findings of Litowski and. Additionally, the spectra are nearly identical to those of E and K without the fluorophores (Figure 2b), showing that the additional fluorescent amino acids do not significantly affect the secondary and quaternary structures of the peptides.

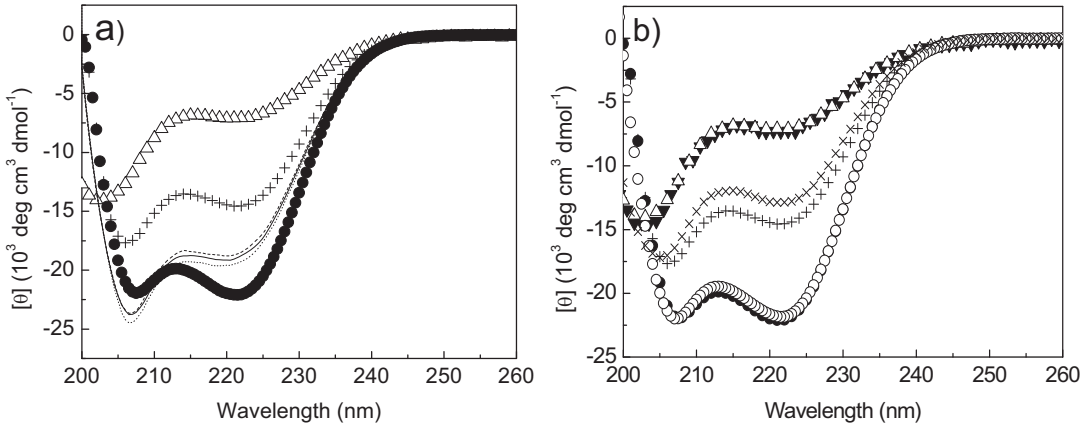

*Figure 2.*a) CD spectroscopic data of E (Δ), K (+), and an equimolar mixture of E and K (●) in PBS. E (- -), K (···), and an equimolar mixture of E and K (—) in 1:1 (v/v) PBS:TFE. b) CD Spectroscopic Data of E (Δ), K (+), and E/K (●) compared to E(-Tyr) (▼), K(-Trp, Gly) (×), and E(-Tyr)/K(-Trp, Gly) (○) in PBS. [Total Peptide] = 200 μM, 25 °C.

Table 1. CD spectroscopic data of the synthetic peptides used in this study.

name[a]	$[\theta]_{222}$		% α-helix[b]		$[\theta]_{222}/[\theta]_{208}$		Coiled coil[c]
	PBS	50% TFE	PBS	50% TFE	PBS	50% TFE	
K	14580	19265	45	60	0.83	0.81	-
E	6662	18472	21	58	0.68	0.80	-
K/E	23308	18760	73	59	1.01	0.81	+

[a] A/B refers to mixtures of the stated compounds with equimolar concentrations. [b] The percentage α-helicity is the ratio of the observed $[\theta]_{222}$ to the predicted $[\theta]_{222}$ for an α-helical peptide of *n* residues x 100. The predicted α-helicity is calculated from $[\theta]_{222}$ = -40 000 x (1-4.6/*n*).[35] [c] The + sign signifies a significant decrease in the $[\theta]_{222}/[\theta]_{208}$ ratio from benign to 50% TFE in PBS, indicative of the folded coiled-coil structure in PBS. [Total Peptide] = 200 μM, 50 mM phosphate, 100 mM KCl, pH 7.0, 25 °C.

FRET spectroscopy

The orientation of the two peptides within the E/K coiled-coil complex was confirmed by measuring the fluorescence resonance energy transfer (FRET) between the donor, tyrosine, on peptide E, and the acceptor, tryptophan, on peptide K. In order to minimize the influence on the peptide structure the natural amino acids tyrosine and tryptophan were used as a FRET pair and introduced them at the ends of the peptides in the **e** position of the heptad repeat. The peptide structure was only nominally modified, as was proven with CD. Both fluorophores are at the N-termini of the peptides, and the Förster distance ($R_o \approx$ 1 nm)[38] is much less than the length of the peptides, which stringently ensures that FRET can only occur when the peptides are in the parallel orientation, not when they are in the antiparallel orientation.

Figure 3 shows emission spectra (excitation at 275 nm) of peptides E and K, E/K in PBS, and E/K in 1:1 PBS:TFE. At 275 nm both tyrosine and tryptophan are excited. In 1:1 PBS:TFE there should be no intermolecular interaction between the peptides (as confirmed with CD), and hence no significant energy transfer between the donor and the acceptor because the distances between them are too great. The spectrum of E/K in 1:1 PBS:TFE in Figure 3 shows contributions from both tyrosine and tryptophan, confirming that there is no FRET between the peptides. In benign buffer the emission spectrum of an equimolar mixture of E and K shows a predominantly K signal. This means that there is efficient energy transfer between the donor (tyrosine) on E and the acceptor (tryptophan) on K, and therefore the peptides E and K form a parallel coiled coil in solution.

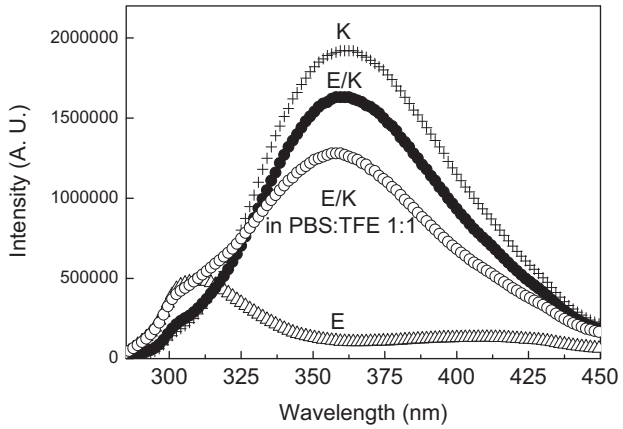

Figure 3. Fluorescence emission spectra of E (Δ), K (+), and an equimolar mixture of E and K (●) in PBS, and in 1:1 (v/v) PBS:TFE (○). [Total Peptide] = 100 μM, 25 °C.

Experimental Results – Binding Properties

Thermodynamic parameters of the thermally and chemically induced equilibrium unfolding were determined by monitoring the resistance of the E/K coiled-coil complex to unfolding as a function of the denaturant GdnHCl concentration, and of increasing temperature.

GdnHCl

The thermodynamic stability of the E/K was determined by measuring the molar ellipticity at 222 nm as a function of GdnHCl concentration. At this wavelength the molar ellipticity is directly proportional to the amount of helical structure.[35] In the folded state, i.e. in benign buffer, the E/K coil is 73% helical. At a GdnHCl concentration of 5.5 M the molar ellipticity at 222 nm of the E/K mixture had dropped to 6% helicity and had stopped decreasing (Figure 4a), indicating that the coiled coil had dissociated and the peptides were predominantly unfolded. The denaturation curve is sigmoidal with a single inflection point, consistent with a two-state equilibrium in which intermediates (folded monomers) are minimally populated at equilibrium.[39] To calculate the conformational stability of the E/K dimer in the absence of denaturant a dimer/monomer equilibrium was used. From the transition zone of the unfolding curve the free energy associated with unfolding as a

function of GdnHCl concentration can be measured, as plotted in Figure 4b. By linear extrapolation to zero GdnHCl concentration the free energy of unfolding at 25 °C in benign buffer was calculated to be 11.7 kcal mol^{-1}.[40] The dissociation constant at 25 °C calculated from this free energy value is 2.5 x 10^{-9} M.

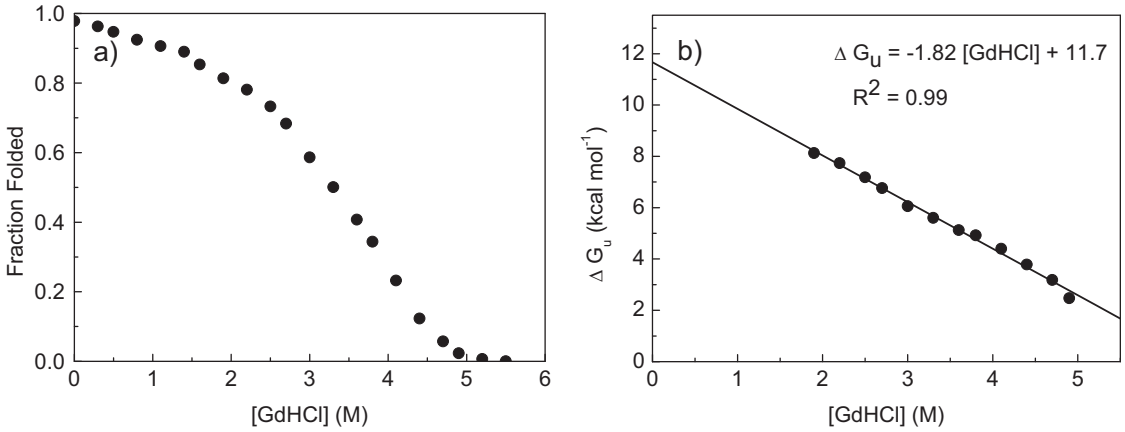

Figure 4. a) GdnHCl unfolding curve of E/K in PBS, 25 °C as followed by CD. The degree of folding in benign buffer is set to fraction folded = 1. [Total Peptide] = 200 μM. b) Gibbs free energy associated with the unfolding of E/K as a function of GdnHCl. The least-squares fit has an intercept of 11.7 kcal mol^{-1}.

Temperature

The thermal denaturation of proteins and peptides provides information about the type and cooperativity of the interactions stabilizing their structures.[39] Figure 5a shows how the folding of the E/K coiled coil changes with temperature. The curve corresponds to a smooth cooperative transition from an α-helical coiled-coil structure to peptides in the random coil conformation. The transition is completely reversed by lowering the temperature. At this concentration the T_m, the temperature at which half of the peptide is in the unfolded form, is 62 °C.

Figure 5c shows that the enthalpy associated with the thermal unfolding of the E/K coiled coil increases linearly with temperature. This is the expected behavior for a two state transition.[41] The gradient of this plot is the change in heat capacity between folded dimers and unfolded monomers.[42] The positive value (0.30 kcal mol^{-1} K^{-1}) of the heat capacity indicates that nonpolar surfaces are being exposed to water upon disassociation of the dimer.[43] It can be concluded that the burial of the bulky non-polar side chains of leucine and isoleucine residues contributes to the stabilization of the E/K dimer as opposed to monomeric peptides.

Using the heat capacity value the change in free energy of unfolding at different temperatures can be calculated (Figure 5d). At 25 °C this value is 11.0 kcal mol^{-1}. This is close to the value of 11.7 kcal mol^{-1} measured using GdnHCl denaturation. The dissociation constant at 25 °C calculated from this ΔG^{H_2O} value is 8.0 x 10^{-9} M.

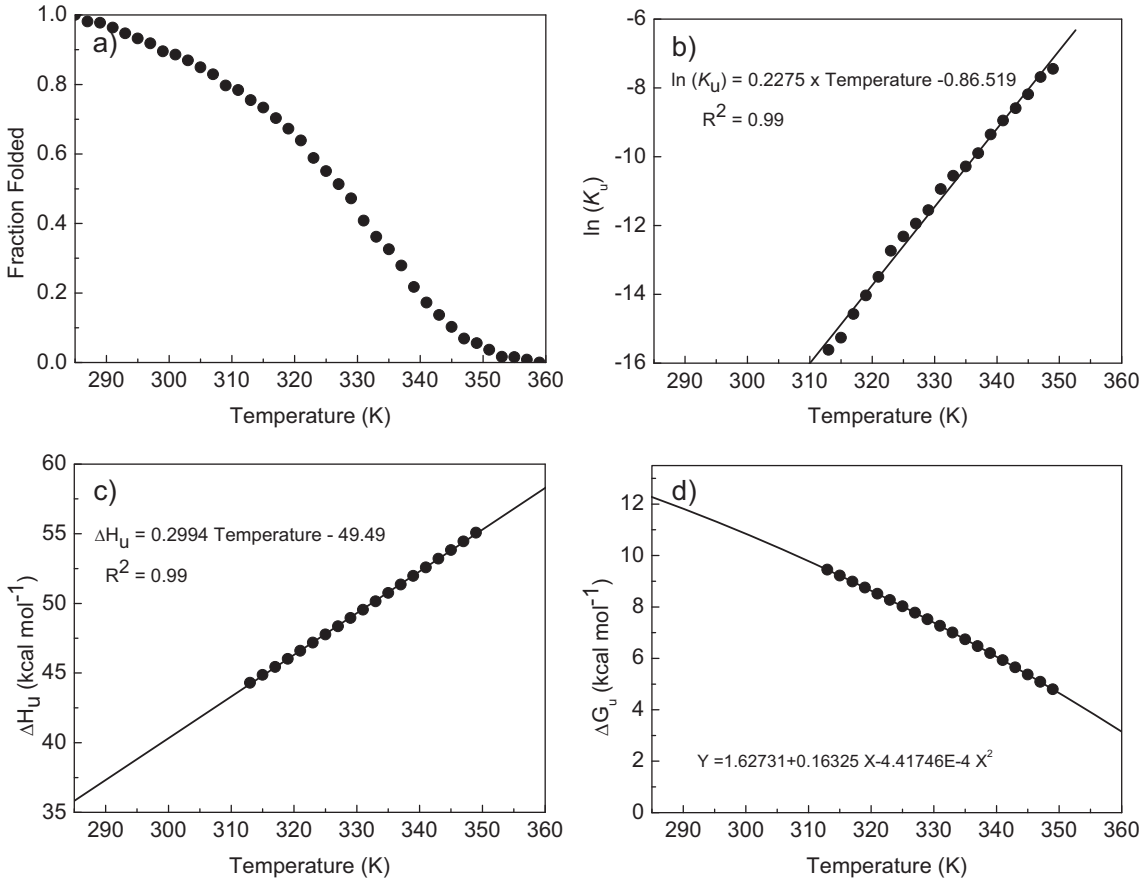

Figure 5. a) Thermal unfolding curve of E/K in 50 mM phosphate, 100 mM KCl, pH 7.0, as followed by CD. [Total Peptide] = 40 μM. b) Van't Hoff plot of the thermal denaturation of E/K. c) Dependence of the enthalpy of unfolding of E/K on temperature. ΔH_u values were obtained using the derivative of the van't Hoff plot. d) Free energy associated with the unfolding of E/K as a function of temperature. The least-squares fit gives a ΔG^{H_2O} value at 25 °C of 11.0 kcal mol^{-1}.

Results of Computer Simulations

The design of the amino acid sequences of E and K, i.e. the placement of amino acids with particular properties at certain positions of the heptad repeat, was based on trends observed experimentally. The E/K coiled-coil interaction has been well characterized on a molecular level: E and K bind to form parallel heterodimers with a free energy of unfolding at 25 °C of ~ 11 kcal mol^{-1}, and a dissociation constant of ~ 10^{-9} M. Molecular dynamics (MD) simulations of the individual peptides and the E/K dimer were then carried out with two goals in mind: first, to see if the structures observed experimentally could be predicted theoretically by the van der Waals and coulomb interactions of the residues; and second, in order to understand in a quantitative way the contributions of the different amino acids to the coiled-coil interaction. If the coiled-coil binding can be understood using MD simulations, sequence designs can be tested for stability before synthesis and characterization.

Structural Properties

For the simulations the experimental conditions were mimicked by immersing the peptides in water with counter ions. Initially, the molecular dynamics of the individual peptides E and K were simulated. Figure 6 shows the starting peptide structures and snapshots at 2 ns. E changes structure significantly over the simulation time, departing from the standard helical structure. K remains largely α-helical, with the largest changes at the N- and C-termini. These results concur with the CD data: both methods demonstrate that E in isolation has a random coil secondary structure, while K is α-helical. This means that the repulsion between the charged glutamic acid side chains in positions **e** and **g** of peptide E is more disruptive to the hydrogen bonding that maintains the α-helicity than the charged lysine side chains in peptide K.

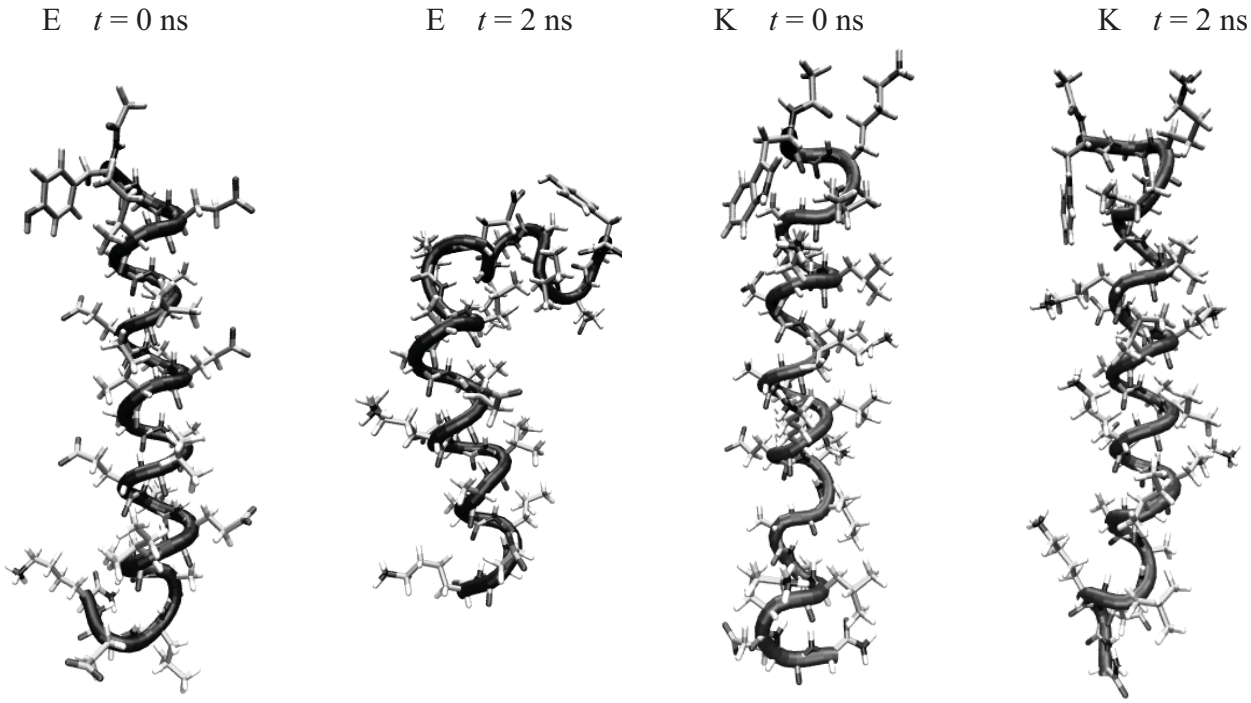

Figure 6. Snapshots of the MD simulations of the peptide monomers in solution. The two left-most Figures shows the initial configuration of peptide E and the final configuration at t = 2.0 ns. The two right-most Figures show the initial configuration of peptide K and the final configuration at t = 2.0 ns. The initial α-helical configurations were constructed in the program Chemsite.[44] Water molecules and counter ions are not shown for simplicity and the backbone is indicated by the blue (E) and red (K) ribbons.

The computed E/K dimer conformation at t = 1.5 ns is shown in Figure 7. Unlike the individual peptides, the structure of the dimer does not alter significantly with time. The peptides are stable as a parallel α-helical dimer, as predicted by the design of the amino acid sequence and as confirmed by circular dichroism, FRET, and also as observed in the structure determined by NMR spectroscopy of IAAL-E3/K3 [27], which have very similar amino acid sequences. As seen in Figure 7b, the peptides interact through the packing

together of isoleucine and leucine residues forming a hydrophobic core away from the water molecules. E and K are staggered, with the C-terminus of peptide K being lower than that of E, again mirroring the results of the structure of IAAL-E3/K3 determined by NMRspectroscopy.[27]

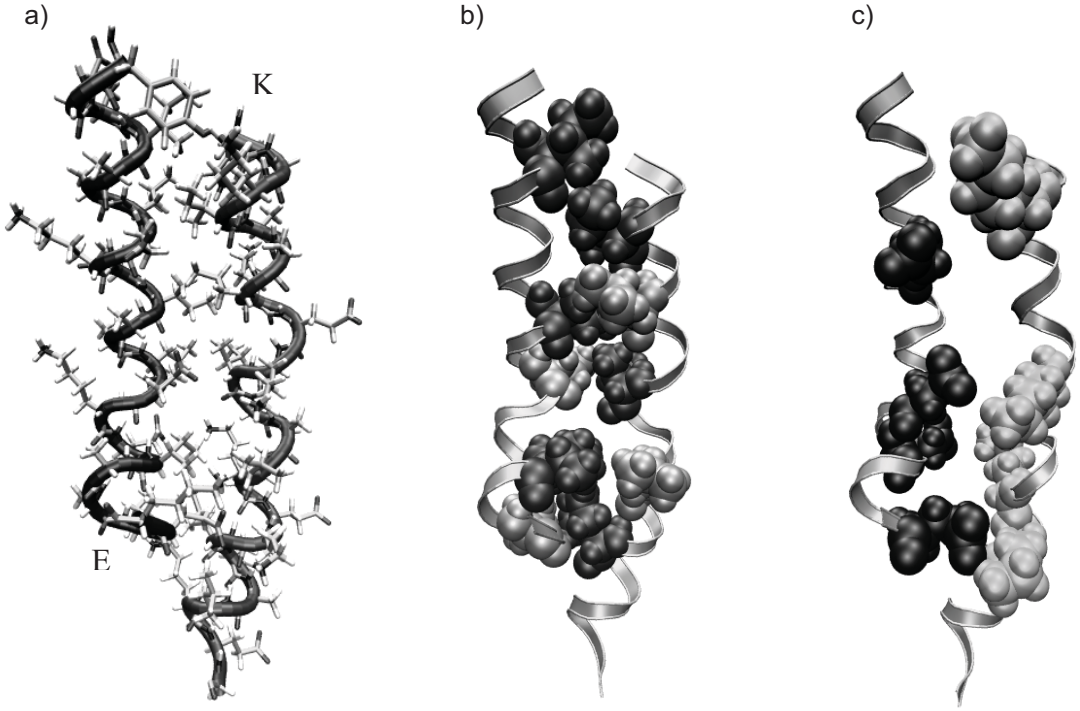

Figure 7. a) Snapshot of the MD simulation of the E-K dimer at t = 1.5 ns. Water molecules are not shown for simplicity and the tubes indicate the peptide backbones. b) Important hydrophobic interactions. Peptide backbones are indicated by the ribbons, isoleucine = dark, leucine = light. c) Important electrostatic interactions. Glutamic acid = dark, lysine = light.

The average tyrosine-tryptophan distance in the heterodimer is 3.5 Å with little variance over the simulation time. This is in agreement with experimental FRET results that revealed that the dimer assumed a parallel orientation.

Core-forming hydrophobic residues

The close-contact intermolecular distances for the core forming leucine and isoleucine residues are shown in Table 2. The close contact pairs are very near one another, on average 2.7 Å, and with little variance over the simulation time. In coiled-coil dimers with parallel conformation the **a** and **a'** residues are purported to pack together in a side-to-side manner, as are the residues at positions **d** and **d'**[45] (Figure 1). In this simulation for the packing of the hydrophobic core, all of the **a** - **a'** distances are less than 3 Å, i.e. the residues are closely packed, but none of the **d** to **d'** distances are less than 3 Å. This means that the helices are slightly twisted from the classical representation of the coiled-coil parallel dimer (Figure 8). All of the possible **a** – (**d**-1)' and **d** – **a**' distances are also within

3 Å. This type of packing is attributed to antiparallel coiled-coil dimers [46], but is also consistent with the 'knobs into holes' core packing model purported by Crick for coiled coils of either orientation.[3] In this model the residues in positions **a** and **d** pack together in a 'knobs into holes' manner, in which each is surrounded by four residues of the opposing strand. The simple "**a** pairs with **a'** and **d** pairs with **d'**" rule does not take into account the close packing of the entire interface.

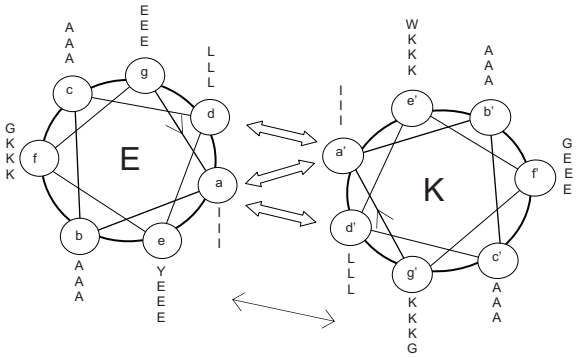

Figure 8. Helical wheel representation of the E/K parallel dimer, with arrows showing the close interhelical distances (< 5 Å) as simulated by molecular dynamics (thin arrow between charged residues, open arrows between residues in the hydrophobic core). Peptides E and K propagate into the page from the N-terminus to the C-terminus.

Core-bordering charged residues

Interhelical salt-bridges ($i \rightarrow i' + 5$ and $i \rightarrow i' + 2$) are often assumed to contribute to the stability of coiled coils. However, taking a cut-off distance of 5 Å for the salt bridges, only four of the ten possible $i \rightarrow i' + 5$, and $i \rightarrow i' + 2$ interactions are present (Table 2). There is some precedent for this: for the peptide pair upon which E and K are based an NMR structure is available, with the authors alleging lysine glutamic acid salt-bridging pairs with the rather long distances of between 9.3 and 16.7 Å.[27,47]. Additionally, fewer intermolecular ion pairs than would be anticipated from the amino acid sequence were observed in the x-ray structure of the extensively studied GCN4 leucine zipper.[45] The fact that in the current simulations only 40% of the distances between glutamic acid and lysine charged side chains are within distances for which salt-bridges are to be expected indicates that the role of charged residues in stabilizing coiled coils is not as extensive as is commonly assumed.

Table 2. The Tyr-Trp intermolecular distance, the close-contact intermolecular hydrophobic distances, and all Glu-Lys distances of the E/K dimer in solution obtained from the MD trajectory. Distances are based on the closest contact interatomic distances between the respective fragments. Averages and standard deviations were taken over the final 500 ps of the trajectory.

E	K	*R* (Å)	Type
1-Tyr	1-Trp	3.5 ± 0.7	
4-Ile	4-Ile	2.9 ± 0.8	a – a'
7-Leu	4-Ile	2.7 ± 0.4	d – a'
11-Ile	7-Leu	2.4 ± 0.2	a – (d-1)'
11-Ile	11-Ile	2.6 ± 0.4	a – a'
14-Leu	11-Ile	2.6 ± 0.6	d – a'
18-Ile	14-Leu	2.6 ± 0.4	a – (d-1)'
18-Ile	18-Ile	2.7 ± 0.4	a – a'
21-Leu	18-Ile	2.8 ± 0.5	d – a'
3-Glu	8-Lys	14.1 ± 1.5	i – i' + 5
8-Glu	3-Lys	2.1 ± 0.6	i – i' + 5
8-Glu	10-Lys	8.6 ± 1.1	i – i' + 2
10-Glu	8-Lys	7.6 ± 0.8	i – i' + 2
10-Glu	15-Lys	12.9 ± 1.1	i – i' + 5
15-Glu	10-Lys	4.1 ± 1.1	i – i' + 5
15-Glu	17-Lys	11.6 ± 0.7	i – i' + 2
17-Glu	15-Lys	4.8 ± 0.9	i – i' + 2
17-Glu	22-Lys	10.4 ± 1.6	i – i' + 5
22-Glu	17-Lys	2.1 ± 0.5	i – i' + 5

The molecular dynamics simulations result in the same peptide intra- and intermolecular structures as observed experimentally, and indicate that the packing of the dimer may be slightly twisted from the classical representation. The large distances between most charged side chains indicate that salt-bridges may not play a major role in stabilizing the dimer. The three dimensional arrangement of peptides is a result of a balance of forces that promote and oppose the compactly folded conformation,[48] and further insights into the peptide binding are obtained by analyzing the energetic contributions to the dimerization.

Binding Properties

The total energy of binding is calculated to be -15.2 kcal mol^{-1}, as shown in Table 3. Although the simulated total binding energy is in the same range as the values obtained from experiments, namely -11.7 kcal mol^{-1} and -11.0 kcal mol^{-1}, it should be noted that only a rough comparison of the values is possible because the simulations lack an entropic term. This would reduce the simulated value, bringing it in the direction of the experimental values. In contrast to the experiments, which gave an overall binding energy, MD simulations also readily allow access to the binding energy components of the different types of residues.

Table 3 breaks down the contribution of each class of residue to the total dimer energy in terms of van der Waals and coulomb energies. It is seen that overall the van der Waals energy is binding, and specifically that the van der Waals interactions of the hydrophobic core-forming isoleucine and leucine residues contribute the most to coiled-coil binding. This supports the conclusion from the temperature induced dimer unfolding that the packing of bulky hydrophobic side chains contributes to the binding energy. In contrast the coulomb energy is non-binding, and the largest anti-binding component is the coulomb repulsion of the glutamic acid and lysine residues. The helix stabilizing residues barely contribute to the overall binding energy; they have the same energy in monomer or dimer form. The 'other' category also contributes to the binding energy, but as seen in the next section this arises from an end-capping moiety, not from amino acid residues.

Table 3. Van der Waals (VdW), coulomb and total contributions to the E/K dimer binding energy grouped per residue type. Hydrophilic: Glu, Lys; hydrophobic: Ile, Leu; helix-stabilizing: Ala, Gly; other: acetyl, Tyr, Trp, NH_2. Grouping of the residues is based on the work by Hodges and Litowski.[28]

Type of Residues	Number of Residues	VdW (kcal mol^{-1})	Coulomb (kcal mol^{-1})	Total (kcal mol^{-1})
Hydrophilic	18	-12.1	23.2	11.1
Hydrophobic	12	-20.0	1.6	-18.4
Helix-stabilizing	15	-0.1	1.2	1.1
Other	6	-3.1	-5.9	-9.0
Total	51	-35.3	20.1	-15.2

In order to probe in more detail the influence of specific residues Table 4 lists the contributions of the van der Waals and coulomb components of each residue to the binding energy of the E/K dimer. The van der Waals interactions are similarly binding for peptides E and K, but E electrostatically destabilizes the dimer while K electrostatically stabilizes it. In isolation E is more random coil than K, and it is seen that the simulated energy changes are greater upon forming a dimer for E rather than K.

Van der Waals Interactions

The van der Waals contribution of amino acids in peptide K, and to some extent E, is dependent on the position along the helix. At the N- and C-termini the van der Waals interactions stabilize dimer binding, and while those in the middle sections destabilize dimer binding, regardless of the position on the helical wheel (Figure 9). It is generally assumed that the middle section of coiled coils are the most stable,[36] but in this case the simulations predict that while the middle sections are the most helical, the most favorable van der Waals interactions in the dimer are the end sections. This reflects the changes in residue packing for different parts of the peptides when going from monomer to dimer form.

Table 4. Van der Waals (VdW), coulomb and total residue contributions to the E/K dimer binding energy. Calculations were obtained from the monomer and dimer MD trajectories and treated according to equations outlined in the computational details.

			E					K		
	Index	Residue	VdW	Coulomb	Total	Index	Residue	VdW	Coulomb	Total
		acetyl	0.3	-0.2	0.1		acetyl	-1.1	0.9	-0.1
e	1	Tyr	-2.2	2.0	-0.2	1	Trp	-0.3	-0.1	-0.4
f	2	Gly	-0.7	0.6	-0.1	2	Gly	-1.1	1.3	0.2
g	3	Glu	-0.7	-0.2	-0.9	3	Lys	-4.1	-3.3	-7.4
a	4	Ile	-1.9	0.1	-1.8	4	Ile	-4.7	1.4	-3.3
b	5	Ala	-0.6	-0.4	-1.0	5	Ala	0.4	-1.1	-0.8
c	6	Ala	-2.2	1.7	-0.4	6	Ala	-0.6	-0.6	-1.2
d	7	Leu	-1.1	-0.5	-1.6	7	Leu	-2.6	1.6	-1.0
e	8	Glu	-2.6	8.4	5.8	8	Lys	1.7	1.4	3.1
f	9	Lys	-1.8	-1.3	-3.0	9	Glu	2.3	-3.2	-0.9
g	10	Glu	-0.3	5.2	4.9	10	Lys	1.8	-0.4	1.4
a	11	Ile	-1.3	0.8	-0.5	11	Ile	0.9	0.1	0.9
b	12	Ala	0.2	-0.9	-0.6	12	Ala	2.4	0.8	3.2
c	13	Ala	0.8	0.7	1.6	13	Ala	2.3	-0.1	2.2
d	14	Leu	1.3	-1.2	0.2	14	Leu	0.3	-0.1	0.2
e	15	Glu	1.1	0.0	1.1	15	Lys	-0.7	1.1	0.4
f	16	Lys	1.3	-0.2	1.2	16	Glu	-0.3	0.8	0.5
g	17	Glu	-0.4	13.7	13.3	17	Lys	-2.8	-1.8	-4.6
a	18	Ile	-1.8	-2.6	-4.4	18	Ile	-4.3	-2.6	-6.9
b	19	Ala	1.1	1.2	2.3	19	Ala	-1.7	-0.1	-1.9
c	20	Ala	2.4	0.8	3.1	20	Ala	-2.9	-2.3	-5.2
d	21	Leu	-2.7	5.4	2.7	21	Leu	-2.0	-0.9	-3.0
e	22	Glu	-4.4	0.4	-4.0	22	Lys	-0.3	1.0	0.7
f	23	Lys	-1.1	-1.1	-2.2	23	Glu	-0.7	2.5	1.8
g		NH_2	0.3	-1.9	-1.6	24	Gly	0.1	-0.4	-0.3
							NH_2	-0.1	-6.6	-6.7
Total			-17.0	30.8	13.8	Total		-18.3	-10.6	-28.9

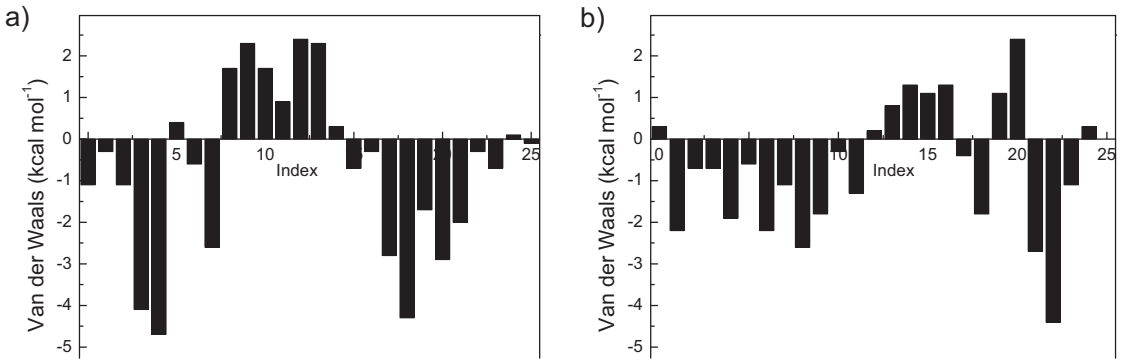

Figure 9. The van der Waals contribution of each residue of peptide K (a), and peptide E (b) to E/K dimer binding.

Coulomb Interactions

It is known that the placement of charged residues along the edge of the hydrophobic core can determine heterodimeric vs. homodimeric peptide association, through destabilizing one quaternary structure.[10] However, whether the electrostatic interactions not only destabilize the homodimeric form, but also stabilize the heterodimeric form is a matter of contention, as is indeed whether salt-bridges form at all.[49, 50] In general for protein and peptide folding electrostatic attraction contributes only moderately to the free energy of folding, while electrostatic repulsion strongly opposes folding.[51] These simulations are in line with this general observation, as there are four detractors to the binding energy that are particularly strong, notably glutamic acid residues at positions **e** and **g**, whereas no amino acid makes a very strong (> -5 kcal mol^{-1}) stabilizing coulomb contribution to the E/K complex formation.

It should be noted that the amide capping moiety at the C-terminus of peptide K displayed the only significant coulomb stabilization (-6.6 kcal mol^{-1}). The C-termini of peptides are often amidated, which it thought to prevent repulsions between charged carboxylic acid termini. In the simulation of the coiled-coil complex the NH_2 group is in close proximity to the carbonyl of alanine in position 20 forming an intramolecular hydrogen-bond that is stable for the duration of the run.

The glutamic acid residues with the highest anti-binding coulomb interactions (positions 8 and 17, 8.4 kcal mol^{-1} and 13.7 kcal mol^{-1} respectively) form close-contacts with charged lysine side-chains (Table 2), but this obviously does not recover the desolvation penalty. Indeed, salt bridges only rarely provide stabilization for protein folding due to under-recovery of desolvation energy.[51] The present simulations find that out of the 10 possible salt-bridges, only 4 are within the distances expected of a salt-bridge, and of the 8 residues involved in these close-contacts only 3 are stabilizing. Therefore in this system the Glu-Lys interaction is important for inferring specificity, i.e. destabilizing homodimers, [52] but does not contribute to stabilizing heterodimers as the majority of the charged side-chains have a lower energy when surrounded by a water solvation shell.

The long-standing hypothesis of the leucine zipper postulates that the sequestering of the hydrophobic residues at positions **a** and **d** drives the dimerization, which is stabilized or destabilized by the placement of charged residues bordering the hydrophobic core.[53] A variation is offered on this: the sequestering of the hydrophobic leucine and isoleucine residues at positions **a** and **d** of E and K drives the dimerization, and heterodimers are destabilized to some extent and homodimers are fully destabilized by the placement of charged glutamic acid and lysine residues bordering the hydrophobic core. This behavior has also been observed for the widely studied stable GCN4 dimer, for which the electrostatic contribution to the dimer was found to be destabilizing using continuum calculations.[54]

By combining experimental work with simulations more detailed information regarding the contribution of specific residues to the stability of the dimer can be obtained. The role of each residue is quantified, and this is not always as one would expect from the coiled-

coil design principles. This allows one to suggest changes in the primary sequence to yield more stable quaternary structures. There is a balance between stability and specificity of coiled-coil dimers, with both positive and negative design being important. Peptide K is energetically more stable as part of the E/K heterocoil than as a monomer (Table 4). There are no residues that have very large destabilizing effects on the dimer. Therefore K seems to be well designed to form E/K heterocoils. If residues were altered to provide greater stability to the E/K heterocoil there would be the danger that K homocoils would be stable. To increase the stability of the heterocoil while maintaining specificity one should focus on the glutamic acid residues of peptide E, which is more stable as a monomer than as a dimer.

CONCLUSIONS

Peptides E and K were designed to form parallel heterodimers in PBS (pH 7.0, 25 °C). K is positively charged and E is negatively charged, and CD experiments show that E is random coil while K is α-helical, i.e. neither can form a homodimeric coiled coil because of charge repulsion. When E and K are combined they interact to form a heterodimeric α-helical coiled-coil complex. FRET experiments revealed that the peptides bind with a parallel orientation. The dissociation energy of the E/K dimer was probed with CD by determining how much energy (temperature or a denaturing salt) is required to disrupt the dimers, and was found to be approximately 11 kcal mol^{-1}. The measured change in heat capacity can be accounted for by burial of bulky leucine and isoleucine non-polar side-chains, therefore experiments predict that stabilization of the dimer is provided by the formation of the hydrophobic core. The computer simulations backed up the experimental results: E is not helical by itself while K is. When combined E and K are in close proximity in the form of a parallel α-helical heterodimer. The binding energy is -15.2 kcal mol^{-1}, with the formation of the hydrophobic core being the largest determinant in the creation of the coiled-coil dimer. In addition to confirming the experimental findings, the computer simulations provide insights into the binding contributions and importance of particular types of amino acids in the peptide sequence.

The largest contribution to the dimer binding energy is the van der Waals interaction of the hydrophobic core-forming residues at the ends of the peptides. It is generally assumed that the middle section of coiled coils are the most stable, but from the simulations it was concluded that the end sections of the dimer have the most favorable van der Waals interactions in comparison to the monomers. Overall the glutamic acid and lysine residues are energetically more stable in monomeric form, and in particular glutamic acid residues display highly unfavorable intra- and interhelical electrostatic repulsions. However, when E and K are in the dimeric form due to the formation of the hydrophobic core the charged residues bordering the hydrophobic core are energetically more stable in close proximity. While the charged amino acids do not contribute overall to the dimer binding, they are important for binding specificity, preventing homodimer formation. The helix stabilizing residues barely contribute to the overall binding energy; they have the same energy in monomer or dimer form.

A challenge in protein and peptide design is to choose a primary structure that will code for particular tertiary and quaternary structures. The largest advances in this area have been in the area of coiled-coil forming peptides.[55] The computational results accurately predicted the oligomerization, direction of coiling, specificity and stability of the coiled-coil tertiary structure, and move beyond the experimental results to quantify the involvement of each amino acid in the peptide sequences. This approach improves the ability to design functional coiled-coil units, widening the scope of their use.

EXPERIMENTAL SECTION

Experimental Details

Materials and Methods

Materials

Fmoc-protected amino acids were purchased from Novabiochem. All other reagents and solvents were obtained at the highest purity available from Sigma-Aldrich or BioSolve Ltd. and used without further purification. Phosphate buffered saline, PBS: 30 mM $K_2HPO_4.3H_2O$, 19 mM KH_2PO_4, 100 mM KCl, pH 7.0.

General Methods

RP-HPLC was performed with a Shimadzu HPLC system with two LC-8A pumps, and an SPD-10AVP UV-VIS detector. Samples were eluted with a linear gradient from A to B, A being 0.1% (v/v) TFA in water, and B acetonitrile. Purification was performed on a Vydac C4 reversed phase column (214TP1022, 22 mm diameter, 250 mm length, 10.00 μM particle size) with a flow rate of 20 mL min^{-1}. Sample elution was monitored by UV detection at 214 nm and 256 nm. For verification of sample purity a reversed phase Vydac C4 column (214TP54, 4.6 mm diameter, 250 mm length, 5.00 μM particle size) was used with a flow rate of 1 mL min^{-1}. Sample elution was monitored by UV detection at 214 nm and 256 nm.

MALDI-TOF mass spectra were acquired using an Applied Biosystems Voyager System 6069 MALDI-TOF spectrometer with an ACH matrix. Samples were dissolved in 1:1 (v/v) 0.1% TFA in water:acetonitrile (TA), at concentrations of ~0.3 mg mL^{-1} for K and E. Solutions for spots consisted of (v/v) 1:10 sample solution: 10 mg mL^{-1} ACH in TA.

^{1}H-NMR spectra were recorded on a Bruker AV-500 spectrometer using the residual proton resonance of deuterated water or acetonitrile for calibration.

Solid-Phase Peptide Synthesis

The peptides E and K were prepared using standard Fmoc chemistry on an Applied Biosystems 431A automated peptide synthesizer. The peptides were synthesized on Sieber-Amide resin. HCTU was used to activate the amino acids derivatives. The peptides were acetylated. Cleavage and deprotection was carried out using 95:2.5:2.5 (v/v) TFA:water:TIS for 1-3 hours. The cleavage mixture and three subsequent rinses of the resin with the TFA mixture were added drop-wise to cold diethylether. The white precipitate was compacted with centrifugation and the supernatant removed. This was repeated three times with the addition of fresh diethylether. The pellets were dried in air or under reduced pressure.

The crude products were purified by RP-HPLC, with gradient elution 35% to 50% B over 20 minutes. After purification all compounds were lyophilized from water to give white material with the following yields: E, K ~40%. The peptides were characterized by MALDI-TOF MS (K: m/z = 2621 $[M+H]^+$, E: m/z = 2544 $[M+H]^+$), RP-HPLC, and ^{1}H-

NMR. For each compound the purity was estimated from RP-HPLC to be greater than 95%.

Characterization of peptide folding

Fluorescence Spectroscopy

Fluorescence measurements were performed using a FS920 fluorometer from Edinburgh Instruments with a DTMS-300X excitation monochromator and a peltier-controlled thermostatic cell. All spectra were obtained at 25 °C using a quartz cuvette with a 1 cm path length. Excitation and emission slits were 5 nm. Emission spectra were measured from 250 nm to 450 nm in 0.5 nm steps at a fixed excitation wavelength of 275 nm. The sampling time was 0.5 s at each wavelength. The spectra were corrected by subtraction of PBS or 50% TFE spectra. The concentration of E or K was 100 μM in each measurement.

Circular Dichroism Spectroscopy

CD spectra were obtained using a Jasco J-815 spectropolarimeter equipped with a peltier-controlled thermostatic cell. The ellipticity is given as mean residue molar ellipticity, [θ] (10^3 deg cm^2 $dmol^{-1}$), calculated by Eqn. (1),

$$[\theta] = (\theta_{obs} \text{ x MRW})/(10\ l\ c) \quad (1)$$

Where θ_{obs} is the ellipticity in millidegrees, MRW is the mean residue molecular weight, l is the path length of the cuvette in cm and c is the peptide concentration in mg/mL.

A 1.0 mm quartz cuvette was used. Spectra were recorded from 260 nm to 200 nm at 25°C. Data was collected at 0.5 nm intervals with a 1 nm bandwidth and 1 s readings. Each spectrum was the average of 5 scans. For analysis each spectrum had the appropriate background spectrum (buffer or 50% TFE) subtracted.

Temperature dependent CD spectra were obtained using an external temperature sensor immersed in the sample. The temperature was controlled with the internal sensor and measured with the external sensor. A 10 mm quartz cuvette was used, and the solutions were stirred at 900 rpm. Spectra were recorded from 260 nm to 200 nm, with data collected at 0.5 nm intervals with a 1 nm bandwidth and 1 s readings. Each spectrum was one scan. The temperature range was 6 °C to 96 °C with a temperature gradient of 2.0 °C/minute and a 60 s delay after reaching the set temperature. The solutions took 5 minutes to return to 6 °C. The spectrum of PBS at 6 °C (average of 5 scans) was subtracted from each spectrum.

The data was analyzed using a two-state unfolding model to determine the fraction folded using Eqn. (2),

$$F_F = ([\theta] - [\theta]_U) / ([\theta]_F - [\theta]_U) \quad (2)$$

Where $[\theta]$ is the observed molar ellipticity, $[\theta]_U$ is the ellipticity of the denatured state, as determined from the plateau of the ellipticity vs. temperature curve, and $[\theta]_F$ is the ellipticity of the folded state at that temperature as determined from a linear fit of the initial stages of the ellipticity vs. temperature curve ($[\theta]_F = -23956 + 131.5$ x T).

The fraction unfolded, F_U, was calculated by Eqn. (3),

$$F_U = (1 - F_F) \quad (3)$$

The dimer dissociation constant in the transition zone was calculated using Eqn. (4),

$$K_U = 2\, P_t F_U^2 / F_F \quad (4)$$

where P_t is the total peptide concentration. By taking the derivative of ln(Ku) vs. Temperature and using this in the van't Hoff equation, Eqn. (5), the change in enthalpy associated with unfolding with temperature can be plotted:

$$\mathrm{d}\ln(K_U) / \mathrm{d}T = \Delta H_U / RT^2 \quad (5)$$

The gradient of this plot ΔC_P, is the difference in heat capacity between the folded and unfolded forms, and can be used in the Gibbs-Helmholtz equation adapted to a monomer-dimer equilibrium, Eqn. (6), to obtain the Gibbs free energy of unfolding as a function of temperature

$$\Delta G_U = \Delta H_m (1 - T/T_m) + \Delta C_p [T - T_m - T\ln(T/T_m)] - RT\ln[P_t] \quad (6)$$

where T_m and H_m, the temperature and enthalpy at the midpoint of the transition, as determined by the maximum of derivative of the ellipticity vs. temperature graph.

The GdnHCl denaturation CD data was obtained by observing the ellipticity at 222 nm in a 1 mm quartz cuvette at 25 °C. Data was collected at 0.5 nm intervals with a 1 nm bandwidth and 1 s readings. Each spectrum was the average of 5 scans.

For data analysis the dimer dissociation constant in the transition zone was calculated in the same way as for temperature denaturation, with $[\theta]_U$ being the ellipticity of the plateau of the ellipticity vs. [GdnHCl] curve and assuming a linear dependency of $[\theta]_F$ with respect to denaturant concentration ($[\theta]_F$ = -1648 + 1314.1 x [GdnHCl]).

The Gibbs free energy of unfolding in the transition zone was calculated using:

$$\Delta G_U = -RT\ln(K_U) \quad (7)$$

ΔG_U decreases linearly with increasing [GdnHCl], so by extrapolating a least-squares fit of

$$\Delta G_U = \Delta G_U^{PBS} - m\,[\mathrm{GdnHCl}] \quad (8)$$

to zero the free energy of unfolding in PBS can be calculated, and from this value the dimer dissociation constant in PBS can be calculated using equation 7.

Computational Details

Binding Energies

For the calculation of the binding energy the potential energy difference between the dimer in solution and the sum of the potential energies of the monomers in solution is computed. The binding energy is defined as follows:

$$\Delta E_{bind}^{E,K} = \left\{\left\langle E_{pot}^{E}\right\rangle + \left\langle E_{pot}^{K}\right\rangle\right\}_{dimer} - \left\{\left\langle E_{pot}^{E}\right\rangle + \left\langle E_{pot}^{K}\right\rangle\right\}_{monomer}. \quad (1)$$

Here $\left\langle E_{pot}^{E}\right\rangle$ denotes the average potential energy of the E-peptide and the accolades indicate the simulation from which the energy values were taken, i.e. either the simulation of the dimer in solution or the simulations of the monomer in solution. In this way one is able to quantify the energetic change when the two peptides form a dimer. The binding

energy can be further split up in terms due the van der Waals, electrostatic and valence interactions. In formulas this would read:

$$\Delta E_{\text{bind}}^{\text{E,K}} = \Delta E_{\text{VdW}}^{\text{E,K}} + \Delta E_{\text{Elec}}^{\text{E,K}} + \Delta E_{\text{valence}}^{\text{E,K}}, \tag{2}$$

where the van der Waals contribution is computed as

$$\Delta E_{\text{VdW}}^{\text{E,K}} = \left\{ \left\langle E_{\text{VdW}}^{\text{E}} \right\rangle + \left\langle E_{\text{VdW}}^{\text{K}} \right\rangle \right\}_{\text{dimer}} - \left\{ \left\langle E_{\text{VdW}}^{\text{E}} \right\rangle + \left\langle E_{\text{VdW}}^{\text{K}} \right\rangle \right\}_{\text{monomer}}. \tag{3}$$

The electrostatic and valence contributions are calculated in the same way as Eqn. (3). In a similar fashion one can write down the separate peptide contributions to the binding energy as

$$\Delta E_{\text{bind}}^{\text{E,K}} = \Delta E_{\text{bind}}^{\text{E}} + \Delta E_{\text{bind}}^{\text{K}}, \tag{4}$$

where

$$\Delta E_{\text{bind}}^{\text{E}} = \left\{ \left\langle E_{\text{pot}}^{\text{E}} \right\rangle \right\}_{\text{dimer}} - \left\{ \left\langle E_{\text{pot}}^{\text{E}} \right\rangle \right\}_{\text{monomer}}, \tag{5}$$

and

$$\Delta E_{\text{bind}}^{\text{K}} = \left\{ \left\langle E_{\text{pot}}^{\text{K}} \right\rangle \right\}_{\text{dimer}} - \left\{ \left\langle E_{\text{pot}}^{\text{K}} \right\rangle \right\}_{\text{monomer}}. \tag{6}$$

The van der Waals and electrostatic energy contributions can be further partitioned among the amino acid residues of the E and K peptides. For example for the E peptide one would get for the van der Waals contribution:

$$\Delta E_{\text{VdW}}^{\text{E}} = \sum_{i=1}^{n} \left[\left\{ \left\langle E_{\text{VdW}}^{i} \right\rangle \right\}_{\text{dimer}} - \left\{ \left\langle E_{\text{VdW}}^{i} \right\rangle \right\}_{\text{monomer}} \right], \tag{7}$$

where the summation runs over all the amino acid residues of the E-peptide.

In practice, for every time frame the energy of the total simulation box is computed and from this is subtracted both the energy of the isolated fragment (i.e. residue or total peptide) and the energy of the simulation box without the fragment. Averages were then taken over the time frames. Since the fragments bear a net charge a simple distance cutoff was used to compute the electrostatic interactions.

Models and Methods

Constant pressure Molecular Dynamics (MD) simulations were performed on the E and K peptides, and on the dimer in aqueous solution using the 1999 release of the AMBER force field.[56, 57] Water was described by the TIP3P water model[58] augmented with a Urey-Bradley cross term. A similar combination of AMBER/TIP3P was recently used by us and other authors in MD simulation studies of a single peptide chain and peptide aggregates in aqueous solution.[59, 60] A cutoff of 9.0 Å was used for all non-bonded interactions and electrostatic interactions were computed using a smooth particle mesh Ewald summation. All calculations were performed with the TINKER software package.[61]

Molecular models of the experimentally used E and K peptides with charged lysine (Lys) and glutamate (Glu) residues were built and minimized with the Chemsite program.[44] It was checked that the resulting structures adopted α-helical conformations. Subsequently, the optimized structures of E and K were both ‘soaked’ into an equilibrated water box

sufficiently large to ensure that periodic images of the peptide did not interact. Water molecules overlapping with the peptide were removed by hand. In the case of the E peptide the edges of the simulation box were 49.6 Å x 35.8 Å x 27.8 Å and the box contained 1523 water molecules. For the K peptide the edges were the same and the number of water molecules was 1506. For every Lys residue along the peptide chain a chloride ion was added to simulation boxes in and for every Glu residue a sodium ion. This ensured that the total net charge of the simulation box was zero in all cases. The initial position of the ion was chosen randomly as long as it did not overlap with the peptide structure or was too close to a water molecule. The pressure was maintained at ambient values by employing the Berendsen barostat.[62] The Beeman algorithm was used to integrate the equation of motion with a time step of 0.5 fs. No intramolecular constraints were employed. The total number of atoms in both simulation boxes is less than 5000, which should result in a fast equilibration of the system. 2.0 ns MD NPT simulations of the E and K peptides in aqueous solution were then performed. Statistical averages were recorded over the final 500 ps of the run.

An initial structure of the dimer of E and K was built with the XMakemol program [63] in such a way that the interstrand Lys-Glu interactions were as favorable as possible. The resulting dimer structure was ‘soaked’ into an equilibrated water box, again ensuring that periodic images did not interact. The resulting box edges were 65.1 Å x 44.6 Å x 37.9 Å and the box contained 3363 water molecules. Initially, a 0.1 ns constraint MD simulation was performed in order to let the peptide dimer adjust to the aqueous water shell. Five interstrand Glu-Lys distances along the backbone were constrained by fixing the CO-HN side-chain interatomic distance to 3.0 Å using a simple flat-welled harmonic potential. After the constraint was released a 1.5 ns MD simulation was performed. Statistical averages were collected over the final 500 ps of the run.

REFERENCES

1. Yu, Y. B. *Adv. Drug Deliv. Rev.* **2002,** 54, (8), 1113-1129.
2. Mason, J. M.; Arndt, K. M. *Chembiochem* **2004,** 5, (2), 170-176.
3. Crick, F. H. C. *Acta Crystallogra.* **1953,** 6, (8-9), 689-697.
4. Schnarr, N. A.; Kennan, A. J. *J. Am. Chem. Soc.* **2003,** 125, (21), 6364-6365.
5. Stevens, M. M.; Allen, S.; Sakata, J. K.; Davies, M. C.; Roberts, C. J.; Tendler, S. J. B.; Tirrell, D. A.; Williams, P. M. *Langmuir* **2004,** 20, (18), 7747-7752.
6. Naik, R. R.; Kirkpatrick, S. M.; Stone, M. O. *Biosens. Bioelectron.* **2001,** 16, (9-12), 1051-1057.
7. Wendt, H.; Leder, L.; Harma, H.; Jelesarov, I.; Baici, A.; Bosshard, H. R. *Biochemistry* **1997,** 36, (1), 204-213.
8. Liu, J. F.; Rost, B. *Protein Sci.* **2001,** 10, (10), 1970-1979.
9. Rose, A.; Meier, I. *Cell. Mol. Life Sci.* **2004,** 61, (16), 1996-2009.
10. Woolfson, D. N., The design of coiled-coil structures and assemblies. In *Fibrous Proteins: Coiled-Coils, Collagen And Elastomers*, Elsevier Academic Press Inc: San Diego, 2005; Vol. 70, pp 79-+.
11. Mason, J. M.; Muller, K. M.; Arndt, K. M. *Biochemistry* **2007,** 46, (16), 4804-4814.
12. Chao, H. M.; Bautista, D. L.; Litowski, J.; Irvin, R. T.; Hodges, R. S. *J. Chromatogra. B* **1998,** 715, (1), 307-329.
13. Li, C. Z.; Plugariu, C. G.; Bajgier, J.; White, J. R.; Liefer, K. M.; Wu, S. J.; Chaiken, I. *J. Mol. Recognit.* **2002,** 15, (1), 33-43.
14. Behncken, S. N.; Billestrup, N.; Brown, R.; Amstrup, J.; Conway-Campbell, B.; Waters, M. J. *J.Biol. Chem.* **2000,** 275, (22), 17000-17007.
15. Pack, P.; Pluckthun, A. *Biochemistry* **1992,** 31, (6), 1579-1584.
16. Petka, W. A.; Harden, J. L.; McGrath, K. P.; Wirtz, D.; Tirrell, D. A. *Science* **1998,** 281, (5375), 389-392.
17. Shen, W.; Zhang, K. C.; Kornfield, J. A.; Tirrell, D. A. *Nat. Mater.* **2006,** 5, (2), 153-158.
18. Wang, C.; Stewart, R. J.; Kopecek, J. *Nature* **1999,** 397, (6718), 417-420.
19. Stevens, M. M.; Flynn, N. T.; Wang, C.; Tirrell, D. A.; Langer, R. *Adv. Mater.* **2004,** 16, (11), 915-918.
20. Ryadnov, M. G.; Woolfson, D. N. *Nat. Mater.* **2003,** 2, (5), 329-332.
21. Zhou, M.; Bentley, D.; Ghosh, I. *J. Am. Chem. Soc.* **2004,** 126, (3), 734-735.
22. Dublin, S. N.; Conticello, V. P. *J. Am. Chem. Soc.* **2008,** 130, (1), 49-+.
23. Potekhin, S. A.; Melnik, T. N.; Popov, V.; Lanina, N. F.; Vazina, A. A.; Rigler, P.; Verdini, A. S.; Corradin, G.; Kajava, A. V. *Chem. Biol.* **2001,** 8, (11), 1025-1032.
24. Lomander, A.; Hwang, W. M.; Zhang, S. G. *Nano Letters* **2005,** 5, (7), 1255-1260.
25. Marsden, H. R.; Korobko, A. V.; van Leeuwen, E. N. M.; Pouget, E. M.; Veen, S. J.; Sommerdijk, N.; Kros, A. *J. Am. Chem. Soc.* **2008,** 130, (29), 9386-9393.
26. Marsden, H. R.; Elbers, N. A.; Bomans, P. H. H.; Sommerdijk, N.; Kros, A. *Angew. Chem., Int. Ed.* **2009,** 48, (13), 2330-2333.
27. Lindhout, D. A.; Litowski, J. R.; Mercier, P.; Hodges, R. S.; Sykes, B. D. *Biopolymers* **2004,** 75, (5), 367-375.
28. Litowski, J. R.; Hodges, R. S. *J. Biol. Chem.* **2002,** 277, (40), 37272-37279.
29. Klok. **2008**.
31. Wagschal, K.; Tripet, B.; Lavigne, P.; Mant, C.; Hodges, R. S. *Protein Sci.* **1999,** 8, (11), 2312-2329.
32. Moitra, J.; Szilak, L.; Krylov, D.; Vinson, C. *Biochemistry* **1997,** 36, (41), 12567-12573.
34. Lyu, P. C.; Liff, M. I.; Marky, L. A.; Kallenbach, N. R. *Science* **1990,** 250, (4981), 669-673.
35. Chen, Y. H.; Yang, J. T.; Chau, K. H. *Biochemistry* **1974,** 13, (16), 3350-3359.
36. Zhou, N. E.; Kay, C. M.; Hodges, R. S. *J.Biol. Chem.* **1992,** 267, (4), 2664-2670.
37. Lau, S. Y. M.; Taneja, A. K.; Hodges, R. S. *J.Biol. Chem.* **1984,** 259, (21), 3253-3261.
38. Eisinger, J.; Feuer, B.; Lamola, A. A. *Biochemistry* **1969,** 8, (10), 3908-&.
39. Boice, J. A.; Dieckmann, G. R.; DeGrado, W. F.; Fairman, R. *Biochemistry* **1996,** 35, (46), 14480-14485.
40. The free energy of dimer unfolding measured by Litowski and Hodges was 9.6 $kcalmol^{-1}$, however, they did not take into account the linear section at the beginning of the denaturation curve. If the current data is treated in the same way a value of 9.2 $kcalmol^{-1}$ is obtained. The glycine, tryptophan and tyrosine residues were added to the peptides investigated by Litowski and Hodges for FRET purposes, and are not designed to contribute to the coiled-coil formation, but were expected not to

disrupt the coiled coil. The similar values of 9.6 and 9.2 kcal mol^{-1} indicate that the effect of the glycine, tryptophan and tyrosine residues is indeed minimal.
41. Privalov, P. L.; Tiktopulo, E. I.; Tischenko, V. M. *J. Mol. Biol.***1979,** 127, (2), 203-216.
42. Defrancesco, R.; Pastore, A.; Vecchio, G.; Cortese, R. *Biochemistry* **1991,** 30, (1), 143-147.
43. Sturtevant, J. M. *Proc. Natl. Acad. Sci. U.S.A.* **1977,** 74, (6), 2236-2240.
44. ChemSW, I. *ChemSite - Computer-Aided Chemistry Modeling*.
45. Oshea, E. K.; Klemm, J. D.; Kim, P. S.; Alber, T. *Science* **1991,** 254, (5031), 539-544.
46. Oakley, M. G.; Hollenbeck, J. J. *Curr. Opin. Struc. Biol.* **2001,** 11, (4), 450-457.
47. The NMR structure was obtained by constraining the Leu Ile distances, which results in closer Lys Glu distances (the distances are greater at the ends of the dimer where there are fewer constraints)
48. Jelesarov, I.; Durr, E.; Thomas, R. M.; Bosshard, H. R. *Biochemistry* **1998,** 37, (20), 7539-7550.
49. Lumb, K. J.; Kim, P. S. *Science* **1995,** 268, (5209), 436-439.
50. Meier, M.; Burkhard, P. *J. Structural Biol.* **2006,** 155, (2), 116-129.
51. Sheinerman, F. B.; Honig, B. *J.Mol. Biol.* **2002,** 318, (1), 161.
52. When the charges of peptides E and K are eliminated (by lowering the pH for E and raising the pH for K) homocoils form, data not shown.
53. McLachlan, A. D.; Stewart, M. *J. Mol. Biol.* **1975,** 98, (2), 293-304.
54. Hendsch, Z. S.; Tidor, B. *Protein Sci.* **1999,** 8, (7), 1381-1392.
55. Chad A. Mirkin, C. M. N., *Nanobiotechnology ll: More Concepts and Applications*. Wiley-VCH: 2007.
56. Cornell, W. D.; Cieplak, P.; Bayly, C. I.; Gould, I. R.; Merz, K. M.; Ferguson, D. M.; Spellmeyer, D. C.; Fox, T.; Caldwell, J. W.; Kollman, P. A. *J. Am. Chem. Soc.* **1995,** 117, (19), 5179-5197.
57. Wang, J. M.; Cieplak, P.; Kollman, P. A. *J. Comp. Chem.* **2000,** 21, (12), 1049-1074.
58. Walser, R.; Hunenberger, P. H.; van Gunsteren, W. F. *Proteins* **2001,** 43, (4), 509-519.
59. Monti, S.; Bronco, S.; Cappelli, C. *J.Phys. Chem. B* **2005,** 109, (22), 11389-11398.
60. Handgraaf, J. W.; Zerbetto, F. *Proteins* **2006,** 64, (3), 711-718.
61. Ponder, J. W. *TINKER - Software Tools for Molecular Design, Version 4.1*, 1990-2003.
62. Berendsen, H. J. C.; Postma, J. P. M.; Vangunsteren, W. F.; Dinola, A.; Haak, J. R. *J. Chem. Phys.* **1984,** 81, (8), 3684-3690.
63. Hodges, M. P. *XMakemol: a program for visualizing atomic and molecular systems, version 5*, 2001.